Electrical Stimulation of Neural Tissue Modeled as a Cellular Composite: Point Source Electrode in an Isotropic Tissue

Omid Monfared, Dragan Nešić, Dean R. Freestone, David B. Grayden, Bahman Tahayori, and Hamish Meffin

Abstract— **Standard volume conductor models of neural electrical stimulation assume that the electrical properties of the tissue are well described by a conductivity that is smooth and homogeneous at a microscopic scale. However, neural tissue is composed of tightly packed cells whose membranes have markedly different electrical properties to either the intra- or extracellular space. Consequently, the electrical properties of tissue are highly heterogeneous at the microscopic scale: a fact not accounted for in standard volume conductor models. Here we apply a recently developed framework for volume conductor models that accounts for the cellular composition of tissue. We consider the case of a point source electrode in tissue comprised of neural fibers crossing each other equally in all directions. We derive the tissue admittivity (that replaces the standard tissue conductivity) from single cell properties, and then calculate the extracellular potential. Our findings indicate that the cellular composition of tissue affects the spatiotemporal profile of the extracellular potential. In particular, the full solution asymptotically approaches a near-field limit close to the electrode and a far-field limit far from the electrode. The near-field and far-field approximations are solutions to standard volume conductor models, but differ from each other by nearly an order or magnitude. Consequently the full solution is expected to provide a more accurate estimate of electrical potentials over the full range of electrode-neurite separations.**

I. INTRODUCTION

The problem of electrical stimulation of neural tissues is particularly important for developing medical bionic devices that use electrical stimulation to either treat a disease, such as deep brain stimulation (DBS), or use it to augment a sense, such as a retinal implant for a bionic eye. Such a model is important because it will facilitate targeted delivery of electrical stimulation, which will lead to selective activation of target neural populations.

In the standard volume conductor approach the tissue is assumed to be homogeneous, even at the microscopic scale, which results in having a local and constant conductivity. However, a real tissue is composed of cells and neurites in which the extracellular and intracellular spaces are separated by a membrane. The membrane has capacitive and high impedance properties and separates the comparatively low resistance intra- and extracellular spaces. The neural tissue is composed of tightly packed fibers creating a high extracellular resistance that constrict the passage of current through the extracellular space. Each fiber in the tissue has a diameter which is wide compared to the width of the extracellular space, resulting in a low resistance intracellular pathway along the full fiber length. However, this current pathway is hard to access due to the existence of the high impedance membrane. None of these facts are accounted in the standard volume conductor models.

Meffin et.al [1] provided a modified framework to the standard volume conductor approach to address these issues. They introduced an admittivity kernel to account for the cellular geometry, which replaces the conductivity used in standard volume conductor models. The admittivity was derived by characterizing the electrical properties of individual neurites via a transimpedance equation. In a further study, they used a mean-field approach to find the admittivity for a composite of neurites [2]. This admittivity changes the spatiotemporal profile of the electrical potentials in a standard volume conductor approach.

In this paper, we apply this framework for modeling the effect of cellular composition of tissue in a volume conductor. The main contribution of the current work is to calculate the admittvity and extracellular electrical potential for a specific tissue type. The tissue is composed of neurites that are crossing each other in all directions representing cortical tissue. For simplicity, we consider an isotropic case of equal probability for neurite directions. We examine how cellular geometry affects the spatial profile of extracellular potential (first stage of the standard volume conductor approach) and how different the profiles are compared to the standard volume conductor approach.

II. METHOD

The volume conductor approach involves both macroscopic and microscopic stages. The first stage calculates the extracellular potential due to a set of electrodes (macroscopic scale). The second stage is to apply the calculation regarding the extracellular potential from stage 1 to an equation to determine the membrane potential (microscopic scale) [1], [3], [4], [5]. Here we perform the stage 1 computations only, which allows us to examine how the cellular composition of tissue affect the spatial distribution of the extracellular potential

We first recall the equations of the standard volume conductor model and then introduce the equivalent equations

This work was funded in part by NICTA Victoria Research Labs.

O. Monfared, D. Nešić, D. R. Freestone, D. B. Grayden, B. Tahayori, and H. Meffin are with the NeuroEngineering Laboratory, Department of Electrical and Electronic Engineering, and O. Monfared and H. Meffin are with NICTA Victoria Research Labs, The University of Melbourne, Parkville, VIC, Australia, 3010, 3002, Australia. See http://www.neuroeng.unimelb.edu.au/ for email addresses.

978-1-4244-7929-0/14/$26.00 ©2014 IEEE

of the cellular composite volume conductor model.

A. Standard volume conductor approach

In the standard volume conductor approach, the current density, $\mathbf{J}_{\rm e}$, and extracellular potential, $V_{\rm e}$, are related via the set of equations:

$$\begin{array}{rcl} \mathbf{J}_{\rm e} & = & -\sigma \nabla V_{\rm e}, \\ \nabla \cdot \mathbf{J}_{\rm e} & = & 0. \end{array} \tag{1}$$

The first equation is called the constitutive equation which relates the current density to the extracellular potential via a constant conductivity, σ. The second equation is the continuity equation for the current density.

Combining these equations and adding a point source term on the right hand side result in Poisson's equation, which describes the distribution of the potential in a tissue:

$$\sigma \left(\frac{\partial^2 V_{\rm e}}{\partial x^2} + \frac{\partial^2 V_{\rm e}}{\partial y^2} + \frac{\partial^2 V_{\rm e}}{\partial z^2} \right) = -\iota(t)\delta(x)\delta(y)\delta(z), \tag{2}$$

where $\delta(\cdot)$ is the dirac function and $\iota(t)$ is the total current coming out of an electrode. When Poisson's equation is solved for this point source electrode, we are given a classical R^{-1} dependency for the decay in potential as a function of space, which is

$$V_{\rm e}(R) = \frac{\iota(t)}{4\pi\sigma R}, \tag{3}$$

where R is the distance from the electrode.

One approach to solve the partial differential equation (2), is to apply the Fourier transform. The following definition is adopted in the application of the Fourier transform.

Definition 1: Fourier transform. The Fourier transform notation of a function $f(\mathbf{p})$ is shown by $\mathcal{F}\{f(\mathbf{p})\}(\mathbf{k})$, where $\mathbf{p} = (x, y, z)$ and $\mathbf{k} = (k_x, k_y, k_z)$. The 3-dimensional spatial Fourier transform pair is defined by

$$\check{f}(\mathbf{k}) = \left(\frac{1}{\sqrt{2\pi}} \right)^3 \int_{R^3} f(\mathbf{p}) e^{-j\mathbf{p}\cdot\mathbf{k}} d\mathbf{p}, \tag{4}$$

$$f(\mathbf{p}) = \left(\frac{1}{\sqrt{2\pi}} \right)^3 \int_{K^3} \check{f}(\mathbf{k}) e^{j\mathbf{p}\cdot\mathbf{k}} d\mathbf{k}. \tag{5}$$

Using Definition 1, the extracellular potential of Equation (2) is represented in the Fourier domain as

$$\hat{\check{V}}_{\rm e}(K) = \frac{\hat{\iota}(\omega)}{(2\pi)^{(\frac{3}{2})}\sigma K^2}, \tag{6}$$

where an ω is the Fourier pair of t (i.e. the angular frequency), $K = |\mathbf{k}|$, and "$\hat{(.)}$" is used to show the temporal Fourier transform. The invrese Fourier transform of this equation was presented in Equation (3).

B. Cellular Composite Model

1) Stage 1: Extracellular Potential Calculation: In the cellular composite volume conductor model, the local extracellular current density is related to extracellular electrical field via convolution in time and space with an admittivity kernel [2].

Consider a tissue comprised of crossing fibers, which are classified by the index $h = 1, \cdots, H$. The local extracellular potential, $V_{\rm e}$, is related to the local current density, $\mathbf{J}_{\rm e,h}$, via a spatiotemporal convolution equation,

$$\mathbf{J}_{\rm e,h} = -\frac{1}{2\pi} \xi_{\rm e,h} \underset{\mathbf{u}_h,t}{*} \nabla V_{\rm e}, \tag{7}$$

$$\mathbf{J}_{\rm e} = \sum_{h=1}^{H} \alpha_h \mathbf{J}_{\rm e,h}, \tag{8}$$

$$\nabla \cdot \mathbf{J}_{\rm e} = 0, \tag{9}$$

where $\xi_{\rm e,h}$ is the admittivity kernel for fibers of type h with both spatial and temporal arguments and is capturing the heterogeneity of tissue at the microscale. The admittivity is defined in such a way to be able to capture some properties of the fibers such as their orientation, diameter, and membrane properties [2]. α_h is the extracellular volume fraction occupied by fibers of type h and $\mathbf{J}_{\rm e}$ is the mean extracellular current density of the tissue. $\mathbf{u}_h$ represents the unit vector parallel to a fiber's axes. The convolution on the direction of $\mathbf{u}_h$ shows the orientation of a class of fiber in the model. The spatial convolution captures the effect of current paths between points in the extracellular spaces via the intracellular space. The capacitive property of the membrane leads to the time convolution. It relates the current density to the extracellular electrical field at previous times.

The cellular composite volume conductor model is defined by Equations (7), (8), (9).

Definition 2: The convolution in Equation (7) is defined as:

$$\begin{array}{rcl} \xi_{\rm e,h} \underset{\mathbf{u}_h,t}{*} \nabla V_{\rm e}(\mathbf{p},t) & = & \int_{-\infty}^{\infty}\int_{-\infty}^{\infty} \xi_{\rm e,h}(s'\mathbf{u}_h, t' : \mathbf{u}_h) \\ & \times & \nabla V_{\rm e}(\mathbf{p} - s'\mathbf{u}_h, t - t') ds' dt'. \end{array} \tag{10}$$

The admittivity kernel, $\xi_{\rm e,h}$, for this general structure is defined in the Fourier domain as [2]

$$\hat{\check{\xi}}_{\rm e,h}(\mathbf{k}, \omega : \mathbf{u}_h) = \hat{\check{\xi}}_{\rm e,T} I_3 + (\hat{\check{\xi}}_{\rm e,L}(\mathbf{k}, \omega : \mathbf{u}_h) - \hat{\check{\xi}}_{\rm e,T}) \mathbf{u}_h \mathbf{u}_h^T, \tag{11}$$

$$\hat{\check{\xi}}_{\rm e,T} = \frac{d}{b\rho_{\rm e}}, \tag{12}$$

$$\hat{\check{\xi}}_{\rm e,L}(\mathbf{k}, \omega : \mathbf{u}_h) = \frac{1}{\rho_{\rm i}} \frac{1 + j\omega\tau_m + (\mathbf{k}\cdot\mathbf{u}_h)^2\lambda_{0J}^2}{1 + j\omega\tau_m + (\mathbf{k}\cdot\mathbf{u}_h)^2\lambda_{0V}^2}, \tag{13}$$

where $\hat{\check{\xi}}_{\rm e,T}$ and $\hat{\check{\xi}}_{\rm e,L}(\cdot)$ are the longitudinal and transverse components of the admittivity $\hat{\check{\xi}}_{\rm e}(\cdot)$. I_3 is the 3×3 identity matrix. $\mathbf{u}_h\mathbf{u}_h^T$ is an outer product. τ_m is the membrane time constant. $\rho_{\rm e}$ and $\rho_{\rm i}$ are the extracellular and intracellular resistivities of the tissue. b is the radius of an ideal cylindrical neurite and d is the thickness of the extracellular sheath (equal to half the width of the extracellular space between neighboring cells). λ_{0J} and λ_{0V} are the electrotonic length constants calculated under current density and voltage boundary conditions for the cable equation [1], respectively, and can be expressed in terms of the fiber's physical parameters,

$$\begin{array}{rcl} \lambda_{0J}^2 & \equiv & \frac{r_{\rm m}}{r_{\rm e}+r_{\rm i}}, \\ \lambda_{0V}^2 & \equiv & \frac{r_{\rm m}}{r_{\rm i}}, \end{array} \tag{14}$$

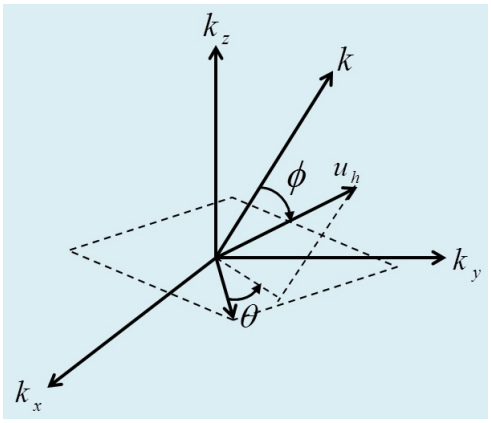

Fig. 1. Spherical polar coordinates. The dotted line projecting $\mathbf{u}_h$ onto the plane is parallel to $\mathbf{k}$ and project onto the plane perpendicular to $\mathbf{k}$. θ is the angle from some arbitrary vector in the plane (dotted parallelogram) perpendicular to $\mathbf{k}$.

where $r_{\rm m} = \frac{R_{\rm m}}{2\pi b}$ is the membrane's unit length resistance. $R_{\rm m}$ is the membrane's unit area resistance and b is the neurite's radius. $r_{\rm e} \approxeq \frac{\rho_{\rm e}}{2\pi b d}$ is the extracellular resistance per unit length where d is the width of the extracellular space and $r_{\rm i} \approxeq \frac{\rho_{\rm i}}{\pi b^2}$ is the intracellular resistance per unit length.

Substituting Equation (7) into Equations (8) and (9) for a point source at the origin, we find

$$\frac{1}{2\pi}\nabla\cdot\Big(\sum_{h=1}^{H}\alpha_h\xi_{\rm e,h}\underset{\mathbf{u}_h,t}{*}\nabla V_{\rm e}\Big) = -\iota(t)\delta(x)\delta(y)\delta(z). \quad (15)$$

Taking a 4-dimensional Fourier transform in time and space and rearranging the terms for $\mathbf{V}_{\rm e}$, the following equation is obtained

$$\hat{\hat{V}}_{\rm e}^{\rm cart}(\mathbf{k}) = \frac{\hat{\iota}(\omega)}{(2\pi)^{3/2}\sum_{h=1}^{H}\alpha_h\mathbf{k}^T\hat{\hat{\xi}}_{e,h}\mathbf{k}}. \quad (16)$$

where $\hat{\hat{V}}_{\rm e}^{\rm cart}$ shows the Fourier transform of the extracellular potential calculated in Cartesian coordinates.

Assumption 1: Fibers have all orientations with equal probability.

Assumption 1 implies a continuous and uniform distribution of fibers' orientations.

We parameterize the fibers' orientations using spherical polar coordinates so that $\mathbf{u}_h$ lies on the unit sphere centered at the origin. The sum over fiber types, $\sum_{h=1}^{H}\alpha_h\mathbf{k}^T\hat{\hat{\xi}}_{\rm e,h}\mathbf{k}$, becomes an integral in the limit of a continuous distribution of fiber orientations,

$$\frac{1}{4\pi}\int_0^{2\pi}\int_0^{\pi}\mathbf{k}^T\hat{\hat{\xi}}_{\rm e}(\mathbf{k},\omega:\mathbf{u}_h)\mathbf{k}\sin\phi d\phi d\theta. \quad (17)$$

The volume fraction α_h becomes a differential area on the surface of the unit sphere $d\alpha = \sin\phi d\phi d\theta/4\pi$, normalized to integral of unity. We choose the spherical polar coordinate system such that axis of rotation is aligned with the vector $\mathbf{k}$. Thus, ϕ is the angle between $\mathbf{k}$ and the unit vector $\mathbf{u}_h$, so that $\mathbf{k}\cdot\mathbf{u}_h = K\cos\phi$. The angle θ is the angle between projection of $\mathbf{u}_h$ onto the plane perpendicular to $\mathbf{k}$, and some arbitrary vector in that plane (see Fig. 1.).

Substituting for $\hat{\hat{\xi}}_{\rm e}(\mathbf{k},\omega:\mathbf{u}_h)$ from Equation (11), the integral in Equation (17) becomes:

$$\begin{aligned}\tfrac{1}{4\pi}\int_0^{2\pi}\int_0^{\pi}\hat{\hat{\xi}}_{\rm e,T}\mathbf{k}^2 &+ \Big(\hat{\hat{\xi}}_{\rm e,L}(\mathbf{k}\cdot\mathbf{u}_h,\omega)-\hat{\hat{\xi}}_{\rm e,T}\Big)\\ &\times (\mathbf{k}\cdot\mathbf{u}_h)^2\sin\phi d\phi d\theta\\ &= g_1K^2\\ &+ \tfrac{g_2}{\lambda_V^2(\omega)}(1-\tfrac{\tan^{-1}(K\lambda_V(\omega))}{K\lambda_V(\omega)}),\end{aligned} \quad (18)$$

where we have used $\mathbf{k}.\mathbf{u}_h = K\cos\phi$ and the approximation $d/b << 1$ to simplify some of the following expressions (assuming $\rho_{\rm i}$ and $\rho_{\rm e}$ have similar magnitudes).

$$\begin{aligned} g_1 &= \tfrac{2}{3}\tfrac{d}{b\rho_{\rm e}} + \tfrac{1}{3}\tfrac{1}{\rho_{\rm i}+\rho_{\rm e}\frac{b}{2d}}\\ &\approxeq \tfrac{4}{3}\tfrac{d}{b\rho_{\rm e}},\\ g_2 &= \tfrac{1}{\rho_{\rm i}}\tfrac{\rho_{\rm e}}{\rho_{\rm e}+\rho_{\rm i}(\frac{2d}{b})}\\ &\approxeq \tfrac{1}{\rho_{\rm i}},\\ \lambda_V(\omega) &= \tfrac{\lambda_{0V}}{\sqrt{1+j\omega\tau_m}}.\end{aligned} \quad (19)$$

In spherical coordinates Equation (16) is represented as:

$$\hat{\hat{V}}_{\rm e}^{\rm sph}(K) = \frac{-jK\hat{\iota}(\omega)}{(2\pi)^{3/2}[g_1K^2+\frac{g_2}{\lambda_V^2(\omega)}(1-\frac{\tan^{-1}(K\lambda_V(\omega))}{K\lambda_V(\omega)})]}, \quad (20)$$

By performing a modified, one dimensional, inverse Fourier transform of Equation (20) with respect to $K = |\mathbf{k}|$, instead of the normal three dimensional inverse Fourier transform with respect to $\mathbf{k}$ we have:

$$V_{\rm e}^{\rm sph}(|R|) = \frac{\mathcal{F}^{-1}\{\hat{\hat{V}}_{\rm e}^{\rm sph}(K)\}}{R}, \quad (21)$$

where, by definition, the function $V_{\rm e}^{\rm sph}(K) = -jKV_{\rm e}^{\rm cart}(\mathbf{k})$, using the observation that dependency on the vector $\mathbf{k}$, occurs only through its norm, K. (Note also, to apply this trick K is allowed vary across the whole real line, including negative values).

To obtain a far-field approximation to Equation (20), we consider the $K > 0$ limit and adopt a Taylor series expansion around $K = 0$ for the $\tan^{-1}(\cdot)$ term. Thus, Equation (20) is estimated as

$$\hat{\hat{V}}_{\rm e}^{\rm FF} = \frac{\hat{\iota}(\omega)}{(2\pi)^{3/2}\sigma_{\rm FF}K^2}, \quad (22)$$

in the far-field limit, where $\sigma_{\rm FF} = g_1+\frac{g_2}{3} \approxeq \frac{4}{3}\frac{d}{b\rho_{\rm e}}+\frac{1}{3\rho_{\rm i}}$ is the conductivity corresponding to the standard volume conductor model in the far-field region. On the other hand, the near-field approximation is achieved when $K\to\infty$. The resulting equation is similar to the far-field Equation (22) but with a conductivity which is different from the far-field conductivity by nearly an order or magnitude,

$$\hat{\hat{V}}_{\rm e}^{\rm NF} = \frac{\hat{\iota}(\omega)}{(2\pi)^{3/2}\sigma_{\rm NF}K^2}, \quad (23)$$

where $\sigma_{\rm NF} = g_1 \approxeq \frac{4}{3}\frac{d}{b\rho_{\rm e}}$ in the near-field region.

TABLE I

PARAMETER VALUE

Parameter	b	d	ρ_{i}	ρ_{e}	R_{m}	τ_{m}
Value	1	0.05	1	1	0.1	1
Unit	μm	μm	$\Omega \cdot$ m	$\Omega \cdot$ m	$\Omega \cdot \mathrm{m}^2$	ms

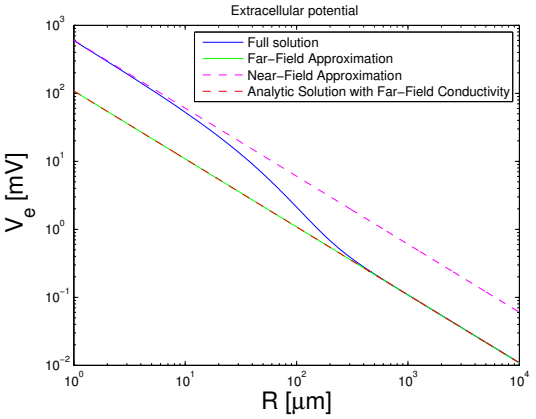

Fig. 2. Blue: Full numerical solution. Green: Far-field approximation using the Taylor series expansion around $K = 0$. Magenta; Near-field approximation. This is the case when $K \to \infty$. Red: The analytic solution for the far-field approximation. The parameters value are given in Table I.

The far-field and near-field equations derived here are both solutions of the standard volume conductor models in the regions, far and close to the electrode, respectively. Here near-field means distances from the electrode much less than the frequency (cf. Equation (3)) dependent electrotonic length constant, $\lambda_V(\omega)$, while far-field means distance much greater.

The Fourier transform inversion of Equations (16), (22), (23) was performed in matlab using ifft function, via the inversion formula in Equation (21). To avoid a numerical instability due the singularity in these expression at $K = 0$, we multiplied the expression by jK (corresponding to differentiation wrt to R) performed the inverse Fourier transform, and then integrated the result wrt R to reverse the effect of the jK multiplication.

III. RESULTS

The results of calculations are plotted in Fig. 2. In this figure, it is shown how the full numerical solution to the cellular composite volume conductor model (blue line) in Equation (16) behaves in the near-field (magenta) and far-field (green) regions. It can be seen that the full numerical solution matches the near-field region in the limit of less than 10 micrometer and then slowly tends toward the far-field region in the limit of greater than one millimeter.

IV. DISCUSSION

In this paper, we modeled the effect of a point source electrical stimulation in an isotropic neural tissue composed of crossing fibers. Under the assumption of "equally oriented fibers in all directions", we derived the tissue admittivity to replace the purely smooth and homogeneous conductivity in the standard volume conductor approach. We then calculated the extracellular potential using the cellular composite model [2]. The results were compared to the solutions of a standard volume conductor model in the near- and far-field regions. The physical intuition behind our calculation was to take into account the effective resistance of the tissue, which is higher close to the electrode. This is due to the current being forced to pass through the tightly packed extracellular space, a fact that has not been taken into account in the conventional model. Taking advantage of the cellular composite model we demonstrated how the cellular geometry affects the spatial profile of extracellular. As a result, we found a range of electrode-neurite separations over which neither approximations (near- or far-field) were able to be applied. This range $(10 - 300\mu m)$ is common in neuroprosthetic and electrophysiological applications.

REFERENCES

[1] H. Meffin, B. Tahayori, D.B. Grayden, and A.N. Burkitt. Modeling extracellular electrical stimulation: I. Derivation and interpretation of neurite equations. *Journal of Neural Engineering*, 9(6):065005, 2012.

[2] H. Meffin, B. Tahayori, E.N. Sergeev, A.N. Burkitt, and D.B. Grayden. Mean field formalism for electrical stimulation of nerve fibre bundles. In *6th Australian Workshop on Computational Neuroscience*, page 51, 2013.

[3] B. Tahayori, H. Meffin, S. Dokos, A.N. Burkitt, and D.B. Grayden. Modeling extracellular electrical stimulation: II. Computational validation and numerical results. *Journal of Neural Engineering*, 9(6):065006, 2012.

[4] D. R. McNeal. Analysis of a model for excitation of myelinated nerve. *Biomedical Engineering, IEEE Transactions on*, (4):329–337, 1976.

[5] B. Coburn. Neural modeling in electrical stimulation. *Critical reviews in biomedical engineering*, 17(2):133–178, 1988.